HHS Public Access

Author manuscript

Ann Biomed Eng. Author manuscript; available in PMC 2017 March 01.

Published in final edited form as:

Ann Biomed Eng. 2016 March ; 44(3): 793–802. doi:10.1007/s10439-015-1507-0.

Development of a High-Throughput Ultrasound Technique for the Analysis of Tissue Engineering Constructs

Jessica Stukel, B.S.[1,*], **Monika Goss, M.S.**[2,*], **Haoyan Zhou, M.S.**[2], **Wenda Zhou, Ph.D.**[1], **Rebecca Willits, Ph.D.**[1,+], and **Agata A. Exner, Ph.D.**[2,3]

Jessica Stukel: js217@zips.uakron.edu; Monika Goss: monika.goss@case.edu; Haoyan Zhou: haoyan.zhou@case.edu; Wenda Zhou: wz20@zips.uakron.edu; Rebecca Willits: willits@uakron.edu; Agata A. Exner: agata.exner@case.edu

[1]Department of Biomedical Engineering, The University of Akron, Akron, OH, 44325, USA

[2]Department of Biomedical Engineering, Case Western Reserve University, Cleveland, Ohio, 44106, USA

[3]Department of Radiology, Case Western Reserve University, Cleveland, Ohio, 44106, USA

Abstract

Development of hydrogel-based tissue engineering constructs is growing at a rapid rate, yet translation to patient use has been sluggish. Years of costly preclinical tests are required to predict clinical performance and safety of these devices. The tests are invasive, destructive to the samples and, in many cases, are not representative of the ultimate *in vivo* scenario. Biomedical imaging has the potential to facilitate biomaterial development by enabling longitudinal noninvasive device characterization directly *in situ*. Among the various available imaging modalities, ultrasound stands out as an excellent candidate due to low cost, wide availability, and a favorable safety profile. The overall goal of this work was to demonstrate the utility of clinical ultrasound in longitudinal characterization of 3D hydrogel matrices supporting cell growth. Specifically, we developed a quantitative technique using clinical B-mode ultrasound to differentiate collagen content and fibroblast density within poly(ethylene glycol) (PEG) hydrogels and validated it in an *in vitro* phantom environment. By manipulating the hydrogel gelation, differences in ultrasound signal intensity were found between gels with collagen fibers and those with non-fiber forming collagen, indicating that the technique was sensitive to the configuration of the protein. At a collagen density of 2.5 mg/mL collagen, fiber forming collagen had a significantly increased signal intensity of $14.90\pm 2.58*10^{-5}$ a.u. compared to non-fiber forming intensity at $2.74\pm 0.36*10^{-5}$ a.u. Additionally, differences in intensity were found between living and fixed fibroblasts, with an increased signal intensity detected in living cells ($5 \pm 0.8*10^{-5}$ a.u. in 1 day live cells compared to $2.26 \pm 0.39*10^{-5}$ a.u. in fixed cells at a concentration of $1*10^{6}$ cells/mL in

[+]To whom correspondence should be addressed: Rebecca Willits, PhD, Department of Biomedical Engineering, The University of Akron, 260 S. Forge St., 301E Olson, Akron, OH 44325-0302, willits@uakron.edu.

[*]These authors contributed equally to this work

Supplemental data:

NMR of PEG-diacrylate

PEG acrylation. The percent completion of PEG-diacrylate was confirmed by NMR. The letters by the PEG-diacrylate structure correspond to the labeled peaks on the NMR spectrum. The PEG-diacrylate was >95% acrylated.

gels containing collagen). Overall, there was a linear correlation >0.90 for ultrasound intensity with increasing cell density. Results demonstrate the feasibility of using clinical ultrasound for characterization of PEG-based hydrogels in a tissue-mimicking phantom. The approach is clinically-relevant and could, with further validation, be utilized to nondestructively monitor *in vivo* performance of implanted tissue engineering scaffolds over time in preclinical and clinical settings.

Key Terms

Ultrasound; imaging; tissue engineering; scaffold; hydrogel; poly(ethylene glycol); collagen

Introduction

Tissue engineering and regenerative medicine are playing increasingly important roles in today's society, with the market potential and financial investment growing accordingly. A survey almost 20 years ago found research and development in this field to be about half a billion dollars with a growth rate of 22% per year[27]. However, new devices face great hurdles in development and FDA approval processes due to the high cost and time for a new product to make it to the market. One such hurdle is the costly preclinical animal study requirement for FDA approval, which often involves sample destruction and results in high batch to batch variability[24, 25, 31]. Because these results are predictive of the performance and safety of biomaterial-based devices upon clinical use, their accuracy and reliability is critical to successful translation of technology. By utilizing noninvasive medical imaging techniques for *in vivo* studies, the cost, required time, and number of animals can be greatly reduced.

The development of biomaterial-based devices, or scaffolds, to support cell growth and function is a key area within tissue engineering and regenerative medicine. Scaffolds are designed to mimic native tissue while providing chemical and mechanical support for cells[20, 32] and can be used for both hard and soft tissue, including bone, cartilage, and wound healing applications[17, 35, 45]. An effective scaffold promotes the intended cellular response, such as proliferation, migration, or differentiation[19]. However, nondestructive evaluation of scaffolds over time, specifically with respect to protein concentration and cell density, remains a challenge. For example, common techniques to quantify protein content include acidic or enzymatic digestion of the scaffold, while to measure proliferation, DNA extraction or metabolic assays destroy the cells[10]. Similarly, for *in vivo* studies, methods to noninvasively or nondestructively monitor the regenerative process are very limited, as most evaluations of the device require the sacrifice of the animal.

Ultrasound is poised to address these challenges as it is a noninvasive, nondestructive imaging technique that is relatively inexpensive. Importantly for translation, ultrasound produces no ionizing radiation, resulting in increased safety for repeated imaging[21]. Ultrasound imaging works by transmitting pulsed sound waves axially from the transducer with a frequency of range of 2–15 MHz[46]. As the ultrasound beam penetrates the tissue or scaffold, some waves are reflected back to the transducer while others continue through the

sample. Waves are reflected when they encounter a boundary of different acoustic impedance and this difference in impedance accounts for the magnitude of the wave[1]. Black and white B-mode images are then formed by encoding the amplitude of the returning wave as a grey-scale value. Ultrasound possesses a high temporal resolution of up to 500 frames per second[46], and for a 12 MHz transducer, which is the frequency for most clinical ultrasound equipment, a spatial resolution of about 200 μm[21]. Previous studies using ultrasound to image various components of tissue regeneration included estimation of cell concentration[29], monitoring cell differentiation and cartilaginous matrix evolution[15, 33], and evaluation of collagen microstructure[30]. However, these studies used high frequency (often 50–100 MHz) small animal ultrasound, which has low penetration depth and is thus not readily translatable to clinical applications where the devices are not implanted superficially.

Clinical ultrasound frequencies have been used to noninvasively characterize biomaterial devices, including correlation of collagen content within cell-containing fibrin scaffolds[26] and quantification of stiffness, volume, and blood supply within injectable chitosan/hydroxyapatite scaffolds over time[8]. Extending the use of clinical ultrasound to characterize cell density and proliferation provides further applicability of the technique for tissue engineering. For example, the measurement of cell density would be crucial to determine the effectiveness of a scaffold to support proliferation and tissue integration. Therefore, the objective of this study was to evaluate the capability of clinical ultrasound to quantify differences in collagen concentration, collagen fiber formation, and fibroblast density in polyethylene glycol (PEG) hydrogels.

Materials and Methods

Materials

Acrylamide, bis-acrylamide, ammonium persulfate (APS), N,N,N′,N′-Tetramethylethylenediamine (TEMED), ethidium homodimer-1, Tris, paraformaldehyde, and phosphate buffered saline (PBS) were purchased from Fisher Scientific, Waltham, MA. Poly(dimethylsiloxane) (PDMS) was made using the Sylgard 184 Silicone Elastomer Kit, Fisher Scientific, Waltham, MA. Dulbecco's Modified Eagle's medium (DMEM) and fetal bovine serum (FBS) were purchased from Sigma Aldrich, St. Louis, MO. Hoechst 33342 and phalloidin-Alexa Fluor 488 were purchased from Life Technologies, Carlsbad, CA. Calcein AM was purchased from Enzo Life Sciences, Irgacure 2959 was received from Ciba Specialty Chemicals, acetic acid was purchased from EMD, ethylenediaminetetraacetic (EDTA) was purchased from Acros Organics, and Trion X-100 was purchased from Ricca Chemical Company. Human dermal fibroblasts were isolated from deidentified tissue obtained from Akron General Medical Center using an approved IRB protocol. Collagen type I was extracted from rat tails according to standard protocols[7, 37] and stored at 4°C in 0.02M acetic acid. PEG-diacrylate was synthesized using a published protocol and verified by NMR [6].

Fabrication and Evaluation of Hydrogels with Collagen

Acid-soluble collagen type I (0–2.5 mg/mL) was mixed into 10% (w/w) PEG-diacrylate (3300 MW) solutions containing Irgacure 2959, PBS, and deionized (DI) water prior to

crosslinking. Two sets of gels were made, one where the collagen was not neutralized (pH 4.0), referred to as non-fiber forming (n=5), and the second where the collagen was suspended in PBS (pH 7.0) to neutralize the acid and permit fiber formation, referred to as fiber forming (n=5). The gels were crosslinked by exposure to ultraviolet light (1.05 mW/cm^2, 365 nm) for 20 min in a Teflon mold between glass slides to form flat rectangular gels. All gels were then cut using a razorblade to form rectangular solids with dimensions of approximately 2×2×4 mm. Following crosslinking, the gels were stored in DI water at 4°C until ultrasound imaging. Collagen organization within the gels was confirmed by reflection microscopy with a 635 nm laser line on a confocal microscope[2]. The emission bandpass was adjusted to 630–670 nm to collect the reflected light from the sample. Images were obtained throughout the depth of the gel.

Ultrasound Imaging of PEG Gels

Imaging—Hydrogel samples were imaged by placing them inside a 10% poly(acrylamide) mold with a recessed trench of approximately 1×1×2 cm filled with water. Acrylamide molds were made using 10% (w/w) solutions of acrylamide and bis-acrylamide (37.5:1 ratio, respectively) in 1X PBS. The solutions were crosslinked via free radical polymerization using 1.7% and 0.1% (v/v) of TEMED and APS, respectively. The molds were polymerized in six well plates around PDMS blocks to create the trench-like void in the gels. The acrylamide gels sat inside a custom-made clay imaging platform that was fixed above the ultrasound transducer. Ultrasound imaging was performed using a clinical ultrasound system (Toshiba Aplio500) with a linear array transducer centered at 12 MHz for B-mode image acquisition (Figure 1). For this transducer setup, the axial beam width was about 0.2 mm and the transaxial beam width was about 1 mm. The mechanical index was set to 0.17, 2D gain was 82, 2D focus depth was 1–2 cm, dynamic range was 60, and images were acquired at 32 frames per second for two seconds. Linear echo power raw data images were stored for analysis. For each set of samples, images were gathered for three different sagittal cross sections. All 64 images in each video clip were analyzed as described below.

Image Analysis—Once all images were acquired, image analysis based on raw signal intensity was conducted using on-board software provided by the scanner manufacturer. Three square 1 mm^2 regions of interest were manually chosen per gel per sagittal cross section image. These regions were selected in the center of the gel to avoid any edge effects, and care was taken to avoid any obvious gel artifacts, such as entrapped bubbles. To enable more robust analysis in these experiments, instead of grey scale pixel values the mean echo power was measured in each region to obtain a spatially averaged intensity value. The raw data values were then averaged for each set of gels and were analyzed with SAS to perform ANOVA and Tukey post hoc tests with $p < 0.05$.

Fabrication and Evaluation of Hydrogels with Cells

Culture—Human dermal fibroblasts were cultured at 37°C and 5% CO_2 in DMEM with 10% FBS. The fibroblasts were encapsulated within PEG gels at 0, 0.1, 0.3, 0.5, and 1×10^6 cells/mL by mixing the cells with 10% (w/w) PEG-diacrylate (3300 MW), Irgacure 2959, and PBS. Non-neutralized 0.1 mg/mL collagen was mixed in the gels cultured for 1 and 6 days. A set of gels was also prepared without collagen to determine if there were

measureable differences in cell spreading after 1 day of culture. Two sets of controls were prepared, one without cells or collagen and a second set with 0.1 mg/mL collagen and no cells. The solution was gelled by exposure to UV light as described above. The mold was turned over every 5 min during gelation to keep the cells suspended within the gel. Crosslinked gels were transferred to well plates and they were either fixed immediately in freshly-made 4% paraformaldehyde or cultured for 1 or 6 days in supplemented media at 37°C and 5% CO_2. The cultured cells were imaged live, fixed in freshly-made 4% paraformaldehyde, and reimaged.

DNA quantification—To quantify the DNA content at 1 and 6 days, the media was aspirated and gels were transferred to 1.5 mL centrifuge tubes. Next, the gels were frozen at −80°C and crushed with a tissue pulverizer. The crushed gels were transferred to centrifuge tubes containing 400 μL Tris-EDTA (TE) (n=5). A standard curve was prepared by suspending 0, 0.1, 0.5, 1, 2.5, or 5×10^5 cells in 400 μL TE and then frozen at −80°C (n=3). The samples were centrifuged for 5 minutes at 5000 rpm to pellet the gel fragments and 200 μL of the supernatant containing the DNA was transferred to separate wells of a 96 well plate. Finally, 100 μL of 10 μg/mL of Hoechst 33342 was added to each well and incubated for 15 min at room temperature. The plate was read on a spectrophotometer (ex/em (nm) 350/461) and the data was averaged after high and low were removed for each sample.

Viability—Cell viability was determined immediately after forming the gels and following 6 days of culture. First, the media was aspirated and the gels were rinsed with PBS. Next, 500 μL of the staining dye containing 2 μM calcein AM, 4 μM ethidium homodimer-1, and 1 μg/mL Hoechst 33342 was added to the well and incubated for 20 min on a rotator at 37°C. Three gels were made for each cell density and 5 images were obtained per gel at 5x on a Zeiss Axiovert fluorescent microscope. Viability was determined by calculating the percentage of cells stained with calcein AM in each image with the ImageJ cell counter[36].

Morphology—To examine the cell morphology, gels containing cells were fixed, permeabilized with 0.5% Triton X-100 for 10 min, quenched with 1 mg/mL sodium borohydride, and blocked with 2 mg/mL bovine serum albumin. The cells were labeled with 100 nM Hoechst 33342 and 100 nM phalloidin-Alexa Fluor 488, labeling the nuclei and actin, respectively. The cells were imaged at 20x. Images were processed using to remove background fluorescence typically found in the DAPI channel with 3D PEG, and overlaid with the green actin images. To better display the overlay, the nuclei were displayed as red.

Statistical Analysis—Data is plotted as average ± standard deviation. All comparisons were performed using a multi-way ANOVA with Tukey post hoc test, considering $p<0.05$ as significant.

Results

Evaluation of hydrogels with collagen

Imaging—B-mode images for both fiber and non-fiber forming collagen resulted in an increased signal intensity with increasing collagen concentration. The white content within each gel on the B-mode images, representing the scatter, increased with increasing collagen

concentration. Fiber forming collagen gels showed greater homogeneity under ultrasound with fewer black or bright areas, and provided higher signal intensity as compared to the non-fiber forming collagen containing gels. (Figure 2). An increasing trend ($p<0.05$) was noted between ultrasound intensity and fiber forming collagen at each concentration, and significant differences were found between gels containing 1.875 and 2.5 mg/mL fiber forming collagen compared to the gels containing non-fiber forming collagen ($p<0.05$) (Figure 2E). Significant differences in signal intensity were seen with increasing collagen concentration, and a detectable range of approximately 625 μg/mL collagen was observed for both non-fiber forming and fiber forming collagen.

Reflection microscopy—To analyze the differences in collagen morphology, confocal reflection images were obtained for the gels with non-fiber forming and fiber forming collagen. Reflection microscopy has been useful in discerning fiber morphology of collagen within scaffolds without labeling[5]. Within the hydrogels imaged, collagen fibers were only visible in fiber forming collagen hydrogels at concentrations of 1.875 and 2.5 mg/mL. Fibers in the gels with 1.875 and 2.5 mg/mL fiber forming collagen were distributed throughout the gel in patches and more fibers were visible with 2.5 mg/mL collagen (Figure 2).

Evaluation of hydrogels with cells

Imaging—Separately from the protein studies, varying concentrations of fibroblasts were seeded in hydrogels to determine if ultrasound could distinguish between different cell densities (Figure 3). After 1 day of culture, the ultrasound signal intensity was measured from gels with and without non-fiber forming collagen. For gels without collagen, the ultrasound signal intensity range was $0.4 \pm 0.01\times10^{-5}$ a.u. to $3.0 \pm 1.2\times10^{-5}$ a.u. for gels with 0 and 1×10^{6} cells/mL living cells, respectively. The only significant difference between living and fixed cells was noted at 0.3×10^{6} cells/mL (Figure 3A). Next, after 1 day of culture with non-fiber forming collagen, the signal intensity was $0.3 \pm 0.07\times10^{-5}$ a.u. and $5.0 \pm 0.8\ x10^{-5}$ a.u. for 0 and 1×10^{6} living cells, respectively (Figure 3B). The intensity for 1×10^{6} live cells in collagen containing gels was significantly greater than either that of living or fixed cells in gels without collagen. The intensity range of fixed cells was consistent in gels with and without collagen. Samples with living cells had a significantly increased intensity for 0.3, 0.5, and 1×10^{6} cells/mL compared to samples with fixed cells cultured for 1 day in collagen containing gels. In the third set of gels, which contained 0.1 mg/mL non-fiber forming collagen and was cultured for 6 days, the only significant difference when examining time in culture was between 1 day and 6 day living cells at 1×10^{6} cells/mL (Figure 3C). The linear regression was determined to be >0.90 for each set of gels. Based on these results, under certain optimized conditions, ultrasound can detect significant differences in as few as 200,000 cells, for example, it is possible to differentiate between live cells at densities of 0.1 and 0.3×10^{6} cells/mL after 1 or 6 days in culture. This number was determined by the minimum statistical difference between neighboring cell densities.

Viability—The viability of the cells was determined at day 0 and day 6 within non-fiber forming collagen scaffolds. At day 0, the cells at each density, 0.1, 0.3, 0.5, and 1×10^{6} cells/mL, were >94±4% viable. After 6 days of culture, the cell viability decreased to

80±4%, 85±3%, 71±5%, and 72±4% (average ± standard deviation), for 0.1, 0.3, 0.5, and 1×10^6 cells/mL, respectively. Live/dead images of day 0 and day 6 viability are shown in Figure A and B. Significant differences were noted between 0.1 and 0.5×10^6 cells/mL between 0 and 6 days for $p<0.05$ as shown in Figure 4C.

DNA quantification—To validate the day 1 and day 6 ultrasound intensities, DNA was extracted and quantified in non-fiber forming collagen containing scaffolds. A standard curve relating DNA concentration to cell number was formed using a quadratic fit, resulting in an r^2 value of 0.96. For each sample group, the no cell control was used as the blank. The average cell number was calculated from this curve, and at Day 1 in collagen containing gels, the result was 1.4×10^5, 1.9×10^5, 1.9×10^5, and 3.7×10^5 cells for 0.1, 0.3, 0.5, and 1×10^6 cells/mL, respectively. These results were not different than Day 0 with collagen or Day 1 without collagen. In addition, the DNA content at day 1 and 6 was not significantly different for each cell density indicating that the cell number did not change during this time (Figure 4D).

Morphology—The cell-containing gels were nuclei labeled with Hoechst 33342 and f-actin was labeled with phalloidin Alexa Fluor 488 to observe the cell morphology. In all gels, the cells remained rounded, but they produced short extensions in gels containing 0.1 mg/mL non-fiber forming collagen as shown in images in Figure 4E. Increasing the cell density did not have a noticeable effect on cell-cell contacts, as most of the cells remained rounded.

Discussion

Several imaging techniques have been explored for nondestructive characterization of biomaterials, including magnetic resonance imaging (MRI)[14, 22], computed tomography (CT)[40, 41], electron paramagnetic resonance (EPR)[22], and ultrasound. Technologies to enhance capabilities of MRI in this area are under rapid development[28], however, because image resolution is proportional to acquisition time[21] and requires the patient to suspend all motion[42], imaging small biomaterial constructs using clinical scanners at sufficiently high temporal and spatial resolution may not be possible. Clinical CT utilizes ionizing radiation and has modest contrast resolution; its resolution is also potentially too low to distinguish changes in non-radiopaque material density at safe radiation doses[16]. In contrast, micro-CT has an enhanced resolution of ~18 μm making it advantageous for examining small specimens with high detail [18,16]. However, micro-CT is not a viable option for longitudinal specimens for *in vivo* imaging in humans as it also emits harmful ionizing radiation[16]. EPR is not typically used clinically due to its high cost, large size, and inability to produce images of the target area[3, 39]. Using a clinically relevant 12 MHz transducer, ultrasound can penetrate about 0.5 cm in soft tissue and the penetration depth is inversely related to the transducer frequency[21], without emitting any ionizing radiation and can therefore be used for longitudinal studies[26]. Ultrasound is advantageous for imaging hydrogels because it provides adequate resolution and is nondestructive. The field of view for ultrasound is limited by the transducer size, however, the transducer is portable and repeated imaging is possible. The wide range of clinically available transducer frequencies makes ultrasound suitable for imaging at many penetration depths, in both *in vitro* and *in vivo* imaging

In this work, clinical ultrasound was investigated as an *in vitro* platform to image protein and cell composition within hydrogels. Collagen was chosen as the model protein for this study because it is common in the extracellular matrix contributing up to 30% of the total protein content in humans and it gives the cells adhesion points as PEG does not allow for significant adhesion[13]. Fibroblasts were chosen as the model cell for this study because they are widely used in wound healing applications and deposit collagen in connective tissue[9, 13, 23]. The results support ultrasound as an imaging modality to reliably quantify protein concentration, fiber organization, and cell density, which are important parameters when evaluating the effectiveness of tissue engineering scaffolds.

When beginning these studies, the protein content was studied first as the baseline control for cell-studies. However, differences were noted with the collagen concentration and extent of fiber formation. Therefore, we further posited that it was not just protein content, but the formation of fibers, that may be detected with ultrasound. Therefore, two different fabrication techniques were used to carefully control the formation of collagen fibers during fabrication. Collagen fibers form readily from acid-soluble collagen at concentrations greater than 0.4 mg/mL, if formed at physiological pH and temperature[44]. However, only pH was controlled in this study with gelation occurring at room temperature, likely leading to minimal fiber formation below 1.8 mg/mL. The formation of fibers was confirmed using reflection microscopy at the higher collagen concentrations. The collagen looked similar to what has been published regarding reflection images of collagen gels,[5] with short linear collagen fibers. However, there is more space between the fibers when they are mixed into the PEG gels rather than forming gels on their own. While reflection microscopy has provided good resolution and a three dimensional (3D) image of collagen fibrillogenesis[2], the technique is not translatable to *in vivo* longitudinal studies.

We were able to achieve a detection limit of approximately 625 μg/mL for both fiber forming and non-fiber forming collagen using clinical ultrasound. Others obtained a spatial resolution of 15 μm, but this result was obtained using a 105 MHz transducer, which is not practical for human use and not widely available[33]. Clinical ultrasound, at 13 MHz, has been used to detect increases in collagen deposition, as measured by hydroxyproline content correlated to gray intensity, over 18 days in scaffolds with myofibroblasts, further supporting ultrasound as an effective technique to detect differences in protein concentration[26]. However, the sensitivity of the technique was not noted. Overall, the sensitivity that we found to both concentration and collagen fibers supports its use as a technique to quantify protein concentration, particularly in longitudinal studies where samples can be tracked over time rather than destroyed for a protein assay. However, further work must be completed to determine how other proteins affect ultrasound signal, particularly proteins that are deposited or reorganized by cells.

In order to use clinical ultrasound for evaluating the performance of tissue engineering scaffolds, detecting changes in cell proliferation and/or morphology is an important characteristic to study. A detection limit of 200,000 cells was achieved with the 12 MHz transducer for fibroblasts under some of the most ideal conditions. The r^2 value, which indicated that the technique was linear, was relatively close to a previously reported r^2 of 0.98 found between cell density and the integrated backscatter coefficient, calculated from

the raw signal intensity in B-mode images with a 30 MHz transducer[29]. The greatest correlation was achieved after 1 day of culture with r^2 values >0.94. Interestingly, we found that the echogenicity was greater for living cells than fixed cells. We hypothesize that our results may be due to the viscoelastic properties of the cell membrane increasing the signal intensity, as the cell membrane is more flexible in live cells compared to their fixed counterparts. Previous works by Czarnota and Kolios used high frequency ultrasound was used to detect cell death and demonstrated that cell death caused changes to cell morphology that resulted in increased backscatter due to nuclei condensation. However, to compare directly to these works is difficult, as the cells in this study were living cells that were fixed into place, rather than cells undergoing programmed cell death. Future work to investigate the ideas that morphology, as well as apoptosis, could lead to signal changes in clinical ultrasound would provide further verification of the results[11, 12]. Further study is necessary to confirm these hypotheses, but would provide an interesting technique to investigate cellular response in hydrogels.

While we measured a change in echogenicity of hydrogels with cells over time for 1×10^6 cells/mL, we found no differences in DNA content between 1 and 6 days for each cell density when quantifying the total DNA. One possible reason for this differential result is related to viability. While the viability was similar to previous reports[34], the cells at day 6 were 72% viable, making the concentration of living cells ~0.72×10^6 cells/mL. This decrease in number of living cells, in combination with some number of non-viable cells, may have caused the reduction in ultrasound signal, making it more similar to the 0.5×10^5 cells/mL. Therefore, ultrasound may be more sensitive to the cell viability than typical DNA quantification techniques, however, this hypothesis should be confirmed by further study.

Overall changes in cell growth were likely limited due to the porosity and stiffness of 10% PEG gels. Previous work has shown minimal cell proliferation and a rounded cell morphology in stiff 3D nondegradable PEG gels because the cells could not overcome the physical barrier formed by the densely crosslinked scaffold[4]. Bott et al. showed that fibroblasts take 1–2 weeks to switch to a stretched morphology in 2.5% (w/v) PEG hydrogels[4], which has approximately 10% the mechanical stiffness of the 10% gels studied here[4, 38]. Additionally, fibroblasts lay down a fibrous matrix in this timeframe towards the end of the proliferative phase of dermal wound healing[13] that may affect cell spreading or proliferation. While ultrasound was capable of measuring cell number over time, the choice of scaffold limited the changes in cell number and morphology seen at day 6. While we have preliminary data that PEG concentration does not influence ultrasound signal intensity, the selection of scaffold to promote cell proliferation or use of techniques to decellularize scaffolds will further validate ultrasound as a viable technique longitudinally.

The technique we propose is not without drawbacks. For example, absorption of the medium, beam diffraction and reverberation artifacts were not directly accounted for in our experiments, but these factors could influence the echogenicity at different depths. Because in a controlled in vitro setup all of the parameters and phantom setup remained constant, these were likely present in all images and thus should not affect overall findings from this work. Along these lines, the current technique utilized a 12 Mhz imaging frequency, which limits the penetration depth and the depth at which implants could be studies *in vivo*.

However, we suggest that this method could be utilized primarily in preclinical development of biomaterials and tissue engineering constructs in animal models. In these cases, the penetration depth should be sufficient. Furthermore, because detection limits would vary in this system depending on transducer frequency, the baseline validation studies would need to be repreated under these different conditions.

In summary, clinical ultrasound provides an attractive noninvasive, nondestructive platform for quantitative imaging of collagen concentration and conformation as well as cell density in 3D tissue engineering scaffolds. These results support the use of clinical ultrasound and this technique has the potential to improve biomaterial imaging in real time. This technique could be used for the creation of predictive models and could be implemented in preclinical and eventually in clinical imaging for rapid longitudinal assessment of implanted tissue engineering scaffolds.

Supplementary Material

Refer to Web version on PubMed Central for supplementary material.

Acknowledgments

This study was supported by the National Institute of Biomedical Imaging and Bioengineering of the National Institutes of Health (R01EB016960 to AAE) and the Margaret F. Donovan Endowment for Women in Engineering (RKW).

References

1. Aldrich JE. Basic physics of ultrasound imaging. Critical Care Medicine. 2007; 35:S131–S137. [PubMed: 17446771]
2. Artym, VV.; Matsumoto, K. Imaging cells in three-dimensional collagen matrix. In: Bonifacino, Juan S., et al., editors. Current protocols in cell biology. Vol. Chapter 10. 2010.
3. Berliner JL, Fujii H. Magnetic resonance imaging of biological specimens by electron paramagnetic resonance of nitroxide spin labels. Science. 1985; 227:517–519. [PubMed: 2981437]
4. Bott K, Upton Z, Schrobback K, Ehrbar M, Hubbell JA, Lutolf MP, Rizzi SC. The effect of matrix characteristics on fibroblast proliferation in 3D gels. Biomaterials. 2010; 31:8454–8464. [PubMed: 20684983]
5. Brightman AO, Rajwa BP, Sturgis JE, McCallister ME, Robinson JP, Voytik-Harbin SL. Time-lapse confocal reflection microscopy of collagen fibrillogenesis and extracellular matrix assembly in vitro. Biopolymers. 2000; 54:222–234. [PubMed: 10861383]
6. Buxton AN, Zhu J, Marchant R, West JL, Yoo JU, Johnstone B. Design and characterization of poly(ethylene glycol) photopolymerizable semi-interpenetrating networks for chondrogenesis of human mesenchymal stem cells. Tissue Eng. 2007; 13:2549–2560. [PubMed: 17655489]
7. Chandrakasan G, Torchia DA, Piez KA. Preparation of intact monomeric collagen from rat tail tendon and skin and the structure of the nonhelical ends in solution. J Biol Chem. 1976; 251:6062–6067. [PubMed: 972153]
8. Chen Y, Li SJ, Li XM, Zhang YC, Huang Z, Feng QL, Zhou ZL, Lin BM, Yu B. Noninvasive Evaluation of Injectable Chitosan/Nano-Hydroxyapatite/Collagen Scaffold via Ultrasound. Journal of Nanomaterials. 2012
9. Chong EJ, Phan TT, Lim IJ, Zhang YZ, Bay BH, Ramakrishna S, Lim CT. Evaluation of electrospun PCL/gelatin nanofibrous scaffold for wound healing and layered dermal reconstitution. Acta Biomaterialia. 2007; 3:321–330. [PubMed: 17321811]

10. Cunha C, Panseri S, Villa O, Silva D, Gelain F. 3D culture of adult mouse neural stem cells within functionalized self-assembling peptide scaffolds. Int J Nanomedicine. 2011; 6:943–955. [PubMed: 21720506]
11. Czarnota GJ, Kolios MC. Ultrasound detection of cell death. Imaging in Medicine. 2010; 2:17–28.
12. Czarnota GJ, Kolios MC, Abraham J, Portnoy M, Ottensmeyer FP, Hunt JW, Sherar MD. Ultrasound imaging of apoptosis: high-resolution non-invasive monitoring of programmed cell death in vitro, in situ and in vivo. British Journal of Cancer. 1999; 81:520–527. [PubMed: 10507779]
13. Diegelmann RF, Evans MC. Wound healing: an overview of acute, fibrotic and delayed healing. Front Biosci. 2004; 9:283–289. [PubMed: 14766366]
14. du Toit LC, Carmichael T, Govender T, Kumar P, Choonara YE, Pillay V. In vitro, in vivo, and in silico evaluation of the bioresponsive behavior of an intelligent intraocular implant. Pharm Res. 2014; 31:607–634. [PubMed: 24002215]
15. Gudur MSR, Rao RR, Peterson AW, Caldwell DJ, Stegemann JP, Deng CX. Noninvasive Quantification of In Vitro Osteoblastic Differentiation in 3D Engineered Tissue Constructs Using Spectral Ultrasound Imaging. Plos One. 2014; 9
16. Guldberg RE, Duvall CL, Peister A, Oest ME, Lin AS, Palmer AW, Levenston ME. 3D imaging of tissue integration with porous biomaterials. Biomaterials. 2008; 29:3757–3761. [PubMed: 18635260]
17. Han Q, Yang P, Wu Y, Meng S, Sui L, Zhang L, Yu L, Tang Y, Jiang H, Xuan D, Kaplan DLP, Kim SH, Tu Q, Chen J. Epigenetically Modified Bone Marrow Stromal Cells (BMSCs) in Silk Scaffolds Promote Craniofacial Bone Repair and Wound Healing. Tissue Eng Part A. 2015
18. Ho ST, Hutmacher DW. A comparison of micro CT with other techniques used in the characterization of scaffolds. Biomaterials. 2006; 27:1362–1376. [PubMed: 16174523]
19. Horii A, Wang X, Gelain F, Zhang S. Biological Designer Self-Assembling Peptide Nanofiber Scaffolds Significantly Enhance Osteoblast Proliferation, Differentiation and 3-D Migration. Plos One. 2007; 2
20. Jensen T, Blanchette A, Vadasz S, Dave A, Canfarotta M, Sayej WN, Finck C. Biomimetic and synthetic esophageal tissue engineering. Biomaterials. 2015; 57:133–141. [PubMed: 25916501]
21. Bushberg, Jerrold TJAS.; Leidholdt, Edwin M., Jr; Boone, John M. The Essential Physics of Medical Imaging. Philadelphia: 2002. p. 473-482.
22. Kempe S, Metz H, Pereira PG, Mader K. Non-invasive in vivo evaluation of in situ forming PLGA implants by benchtop magnetic resonance imaging (BT-MRI) and EPR spectroscopy. Eur J Pharm Biopharm. 2010; 74:102–108. [PubMed: 19545625]
23. Kim HN, Hong Y, Kim MS, Kim SM, Suh KY. Effect of orientation and density of nanotopography in dermal wound healing. Biomaterials. 2012; 33:8782–8792. [PubMed: 22959181]
24. Kim K, Jeong CG, Hollister SJ. Non-invasive monitoring of tissue scaffold degradation using ultrasound elasticity imaging. Acta Biomaterialia. 2008; 4:783–790. [PubMed: 18348913]
25. Kim SH, Lee JH, Hyun H, Ashitate Y, Park G, Robichaud K, Lunsford E, Lee SJ, Khang G, Choi HS. Near-infrared fluorescence imaging for noninvasive trafficking of scaffold degradation. Sci Rep. 2013; 3:1198. [PubMed: 23386968]
26. Kreitz S, Dohmen G, Hasken S, Schmitz-Rode T, Mela P, Jockenhoevel S. Nondestructive Method to Evaluate the Collagen Content of Fibrin-Based Tissue Engineered Structures Via Ultrasound. Tissue Engineering Part C-Methods. 2011; 17:1021–1026. [PubMed: 21663456]
27. Lysaght MJ, Nguy NA, Sullivan K. An economic survey of the emerging tissue engineering industry. Tissue Eng. 1998; 4:231–238. [PubMed: 9836788]
28. Ma D, Gulani V, Seiberlich N, Liu K, Sunshine JL, Duerk JL, Griswold MA. Magnetic resonance fingerprinting. Nature. 2013; 495:187–192. [PubMed: 23486058]
29. Mercado KP, Helguera M, Hocking DC, Dalecki D. Estimating Cell Concentration in Three-Dimensional Engineered Tissues Using High Frequency Quantitative Ultrasound. Annals of Biomedical Engineering. 2014; 42:1292–1304. [PubMed: 24627179]

30. Mercado KP, Helguera M, Hocking DC, Dalecki D. Noninvasive Quantitative Imaging of Collagen Microstructure in Three-Dimensional Hydrogels Using High-Frequency Ultrasound. Tissue Eng Part C Methods. 2015
31. Perrin S. Make mouse studies work. Nature. 2014; 507:423–425. [PubMed: 24678540]
32. Ribeiro VP, Almeida LR, Martins AR, Pashkuleva I, Marques AP, Ribeiro AS, Silva CJ, Bonifacio G, Sousa RA, Reis RL, Oliveira AL. Influence of different surface modification treatments on silk biotextiles for tissue engineering applications. J Biomed Mater Res B Appl Biomater. 2015
33. Rice MA, Waters KR, Anseth KS. Ultrasound monitoring of cartilaginous matrix evolution in degradable PEG hydrogels. Acta Biomaterialia. 2009; 5:152–161. [PubMed: 18793879]
34. Salinas CN, Anseth KS. The influence of the RGD peptide motif and its contextual presentation in PEG gels on human mesenchymal stem cell viability. J Tissue Eng Regen Med. 2008; 2:296–304. [PubMed: 18512265]
35. Sancho-Tello M, Forriol F, Gastaldi P, Ruiz-Sauri A, Martin de Llano JJ, Novella-Maestre E, Antolinos-Turpin CM, Gomez-Tejedor JA, Gomez Ribelles JL, Carda C. Time evolution of in vivo articular cartilage repair induced by bone marrow stimulation and scaffold implantation in rabbits. Int J Artif Organs. 2015
36. Schneider CA, Rasband WS, Eliceiri KW. NIH Image to ImageJ: 25 years of image analysis. Nature Methods. 2012; 9:671–675. [PubMed: 22930834]
37. Silver FH, Trelstad RL. Type I collagen in solution. Structure and properties of fibril fragments. J Biol Chem. 1980; 255:9427–9433. [PubMed: 7410433]
38. Skornia SL, Bledsoe JG, Kelso B, Kuntz Willitz R. Mechanical properties of layered poly (ethylene glycol) gels. J Appl Biomater Biomech. 2007; 5:176–183. [PubMed: 20799187]
39. Solorio L, Babin BM, Patel RB, Mach J, Azar N, Exner AA. Noninvasive characterization of in situ forming implants using diagnostic ultrasound. J Control Release. 2010; 143:183–190. [PubMed: 20060859]
40. Szymanski-Exner A, Stowe NT, Lazebnik RS, Salem K, Wilson DL, Haaga JR, Gao J. Noninvasive monitoring of local drug release in a rabbit radiofrequency (RF) ablation model using X-ray computed tomography. J Control Release. 2002; 83:415–425. [PubMed: 12387949]
41. Szymanski-Exner A, Stowe NT, Salem K, Lazebnik R, Haaga JR, Wilson DL, Gao J. Noninvasive monitoring of local drug release using X-ray computed tomography: optimization and in vitro/in vivo validation. J Pharm Sci. 2003; 92:289–296. [PubMed: 12532379]
42. Uyanik I, Lindner P, Tsiamyrtzis P, Shah D, Tsekos NV, Pavlidis IT. Applying a Level Set Method for Resolving Physiologic Motions in Free-Breathing and Non-gated Cardiac MRI. Functional Imaging and Modeling of the Heart. 2013; 7945:466–473.
43. Varslot T, Krogstad H, Mo E, Angelsen BA. Eigenfunction analysis of stochastic backscatter for characterization of acoustic aberration in medical ultrasound imaging. J Acoust Soc Am. 2004; 115:3068–3076. [PubMed: 15237831]
44. Willits RK, Skornia SL. Effect of collagen gel stiffness on neurite extension. J Biomater Sci Polym Ed. 2004; 15:1521–1531. [PubMed: 15696797]
45. You JO, Rafat M, Almeda D, Maldonado N, Guo P, Nabzdyk CS, Chun M, LoGerfo FW, Hutchinson JW, Pradhan-Nabzdyk LK, Auguste DT. pH-responsive scaffolds generate a pro-healing response. Biomaterials. 2015; 57:22–32. [PubMed: 25956194]
46. Zhou H, Hernandez C, Goss M, Gawlik A, Exner AA. Biomedical Imaging in Implantable Drug Delivery Systems. Curr Drug Targets. 2014

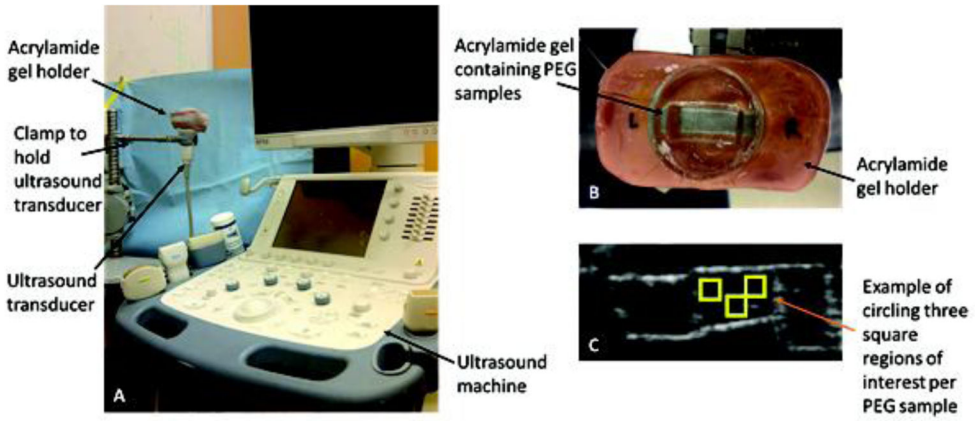

Figure 1.

Experimental setup. (A) Ultrasound imaging setup showing the custom made PEG hydrogel holder fixed above the transducer. (B) Custom made imaging platform consisting of a water-filled acrylamide mold containing PEG hydrogel samples. (C) Sample output image: for each set of samples, images were gathered for three different sagittal cross sections, and three regions of interest were manually chosen for each gel in the image.

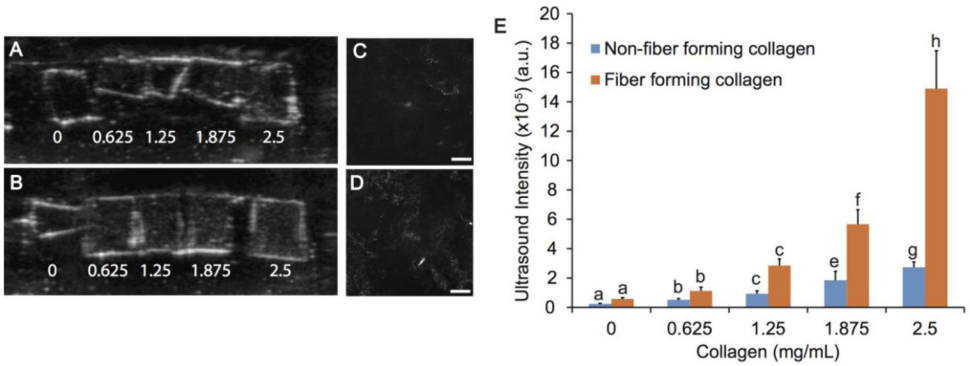

Figure 2.

Ultrasound imaging of PEG gels with various concentrations of collagen. Both non-fiber forming (A) and fiber forming (B) collagen was added in concentrations ranging from 0 to 2.5 mg/mL. The borders of each gel appear white due to the gel-water interface. There is a visible gradient for fiber-forming collagen, which correlates well to the quantitative intensity values. Collagen fibers were observed in confocal reflectance microscopy images of (C) 1.875 and (D) 2.5 mg/mL fiber forming collagen in PEG gels at 10x. No reflection was found in PEG gels with non-fiber forming collagen at any concentration. Scale bar = 200 μm. (E) Ultrasound signal intensity from B-mode images of PEG gels with 0–2.5 mg/mL non-fiber forming or fiber forming collagen. Statistical groups are indicated by lowercase letters with each letter indicating groups that are statistically similar. A significant increase in intensity for 1.875 and 2.5 mg/mL fiber forming collagen as compared to non-fiber forming collagen at each concentration ($p<0.05$).

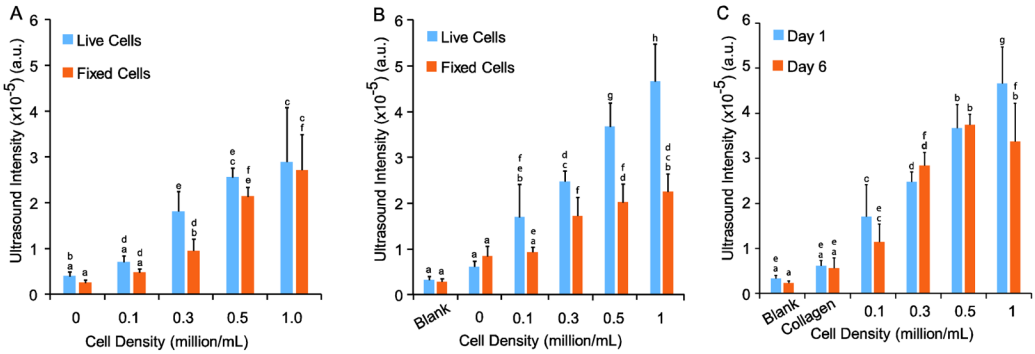

Figure 3.

Ultrasound imaging of PEG gels with 3D embedded fibroblasts. Both living and fixed cells were imaged after 1 day in gels (A) without collagen and (B) with 0.1 mg/mL non-fiber forming collagen. For B and C, blank refers to gels without collagen or cells. Statistical groups are noted by lowercase letters with each letter indicating groups that are statistically similar within each graph. Differences were found for living cells between 0.1, 0.3, and 1×10^6 cells/mL without collagen and between 0, 0.1, 0.3, 0.5, and 1×10^6 cells/mL with collagen. Fewer differences were noted with fixed cells. After 6 days of culture (C), differences in living cultures were found between no cells and concentrations above 0.3×10^6 cells/mL.

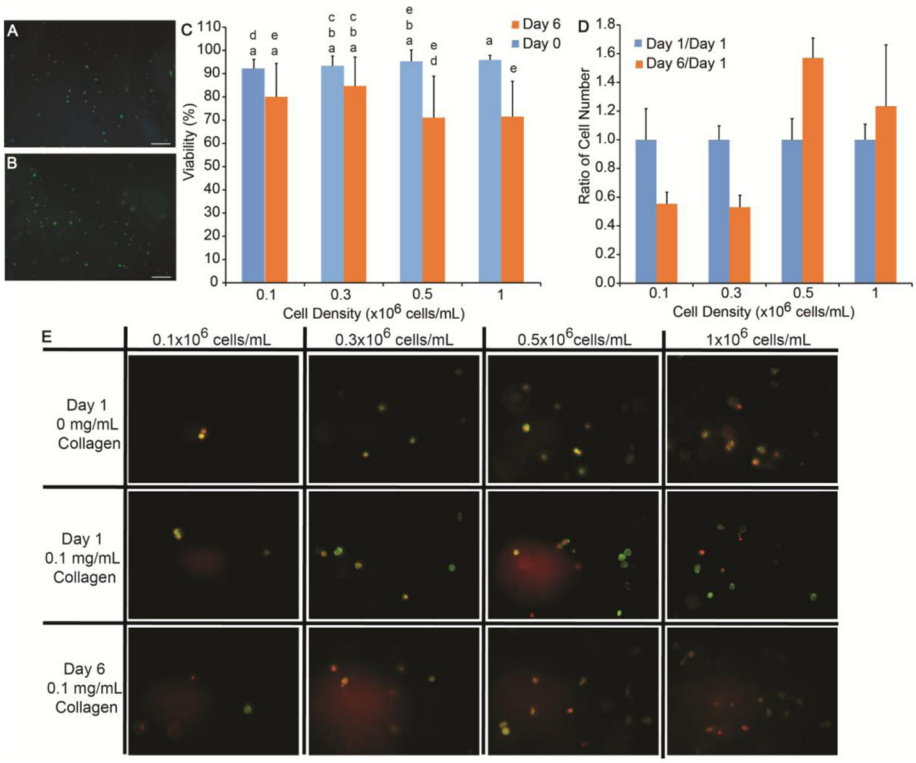

Figure 4.

Verification of cultures with traditional methods. Viability of the cell cultures in PEG gels was confirmed at both (A) 0 and (B) 6 days. Scale bars indicate 200 μm. The images were quantified using the number of viable cells (green) and total cells (blue) and was 94% after encapsulation and 72% after 6 day. Statistical groups are noted by lowercase letters with each letter indicating groups that are statistically similar. Differences were found between days 0 and 6 for 0.5 and 1×10^6 cells/mL (C). (D) The number of cells at Day 6 was quantified by DNA extraction to was normalized to Day 1. No statistical differences were noted. (E) Finally, fibroblast morphology was examined using Hoechst 33342 (displayed as red) and phalloidin Alexa Fluor 488, labeling the nuclei and f-actin, respectively. Fibroblasts were cultured at varying cell density for 1 day with 0 or 0.1 mg/mL collagen and for 6 days with 0.1 mg/mL collagen. All cells maintained a rounded morphology. Scale bar = 50 μm.